The effects of urban vehicle traffic on heavy metal contamination in road sweeping waste and bottom sediments of retention tanks

Nicole Nawrot [a],*, Ewa Wojciechowska [a], Shahabaldin Rezania [c], Jolanta Walkusz-Miotk [b], Ksenia Pazdro [b]

[a] *Gdańsk University of Technology, Faculty of Civil and Environmental Engineering, Narutowicza 11/12, 80-233 Gdańsk, Poland*
[b] *Institute of Oceanology of the Polish Academy of Sciences, Marine Geotoxicology Laboratory, Powstańców Warszawy 55, 81-712 Sopot, Poland*
[c] *Department of Environment and Energy, Sejong University, Seoul 05006, South Korea*

HIGHLIGHTS

- Tracking connection between used car parts and heavy metals in bottom sediments
- Mechanical waste from car diagnostics and road sweeping wastes as heavy metal sources
- Multivariate statistics, flag element ratio and Pb isotope ratios applied as tools
- Vehicles during use supplement Zn, Cu, Ni and partly Cr.
- Pb in urban retention tank sediments originates mainly from coal combustion.

GRAPHICAL ABSTRACT

ARTICLE INFO

ABSTRACT

Diffuse pollution formed during a surface runoff on paved surfaces is a source of heavy metals (HMs) of various origin. This research study indicates the connection between bottom sediments of retention tanks located on urban streams and road sweeping wastes (RSW) that migrate during surface runoff to the stormwater drainage systems with discharge to the retention tanks. Moreover, we test the primary sources of HMs in RSW by analysing the mechanical wastes (MW) produced by vehicles in order to track the relationship between car parts and HMs deposited in the retention tanks receiving the surface runoff from streets. To identify the origin of HMs diverse source tracking approaches were used: statistical methods, Pb isotope ratios, and the flag element ratio approach. MW presented a very high HMs content (max observed values in mg/kg d.w.: 10477-Zn, 3512-Cu, 412-Pb, 3.35-Cd, 226-Ni, and 633-Cr), while for RSW the HMs content was similar to the bottom sediments. The total carcinogenic risk raises concerns due to the Cr content. The source of Zn was tyre wear and traffic. Ni, Cr, Fe, and Cd were correlated to Zn and shared a common/similar origin. PCA suggested that Cu features quasi-independent behaviour. The Pb isotopic ratios of RSW indicated Pb enrichment originating from coal combustion, while the gasoline and diesel source of Pb was excluded. The Pb isotopic ratios characteristic for MW were in within the following ranges: 1.152–1.165 ($^{206}Pb/^{207}Pb$), 2.050–2.085 ($^{208}Pb/^{206}Pb$), and 2.350–2.418 ($^{208}Pb/^{207}Pb$). The complex analysis of HMs origin confirmed the motorization origin of HMs: Zn, Cr, Ni, and Cd, except Pb (coal combustion as the main source) and Cu (non-uniform origin). The results of various source tracking methods were coherent, but Pb isotope ratios alone brought important information allowing to link Pb in sediments to the atmospheric deposition of coal combustion products.

* Corresponding author.
 E-mail address: nicnawro@pg.edu.pl (N. Nawrot).

1. Introduction

Surface runoff in developed cities is a source of an uncontrolled amount of pollution transported to stormwater drainage systems. As a result, surface runoff supplies the surface waters directly (or indirectly by stormwater channels) and undermines their safe use due to increased toxicity, which poses ecological and human health risks. Among the hazardous elements, heavy metals (HMs) play an important ecological role, due to their toxicity, abundance, and non-degradability (Islam et al., 2015a, 2015b). HMs are bound to suspended solids transported along with the stormwater and may deposit in the bottom sediments of receivers. In the cities, the important aspects of stormwater infrastructure management are retention tanks which decrease the peak outflows and protect the cities from flooding during torrential rainfalls. The reduced flow velocities in the retention tanks favor sedimentation of the solids washed off from the urban streets by surface runoff (Sojka et al., 2018). The city's footprints are visible in the bottom sediment pollution degree which usually exhibits different levels of contamination in comparison to the geochemical background. In general, non-point sources of pollution are underestimated in the assessment of the general pollution scenario, as well as harder to control. This results directly from the nature of dispersed pollution as there is no "end-of-pipe" hot spot (Zafra et al., 2017).

Car traffic is mentioned first among HM sources in urban areas, but there are hardly any studies that present comprehensive quantitative assessments (Adamiec et al., 2016). Many kinds of research put attention to road dust as an important component of the urban ecological system (Men et al., 2018). During dry periods considerable range of HMs from vehicle activities usually build-up on roads and junctions (Zafra et al., 2017). Then, during precipitation, these pollutants can be washed-off by stormwater runoff and deposited in the stormwater drainage system or receivers. The pollutant load flushing with surface runoff and transported by stormwater drainage system to receivers is conditioned by seasonal changes, such as dry and wet periods, snowmelt, or the content of organic matter related to urban vegetation (Sojka et al., 2018). Street dust is supplemented with HMs due to car exhaust emission as well as wear and tear of vehicle parts such as tyres and brake discs (Yuen et al., 2012). The source of the toxic elements are the fluids released from vehicles onto the surface of the street. Moreover, street dust contains HMs originating from the ground or overhead lines used by trams, trolleybuses, and trains (Zgłobicki et al., 2019). The most widespread and documented elements include Zn, Cd, Cu, Pb, Ni, Cr, as well as Co and Hg (Shi et al., 2011; Zgłobicki et al., 2019). The particle properties used in the automotive industry are difficult to characterise because every year numerous new materials are introduced onto the market. The number of materials used in braking systems is difficult to estimate, since more than 100 formulations of patented friction materials have been introduced during the last 4 decades (Adamiec et al., 2016). Zn, Cr, Ni, Cd could be emitted from brake wear, motor oil, and tyre wear; therefore, this element is common in areas with high volumes of traffic (Ferreira et al., 2016). Crosby et al. (2014) ascribe Zn and Cu potential deposition to brake linings and tyre wear. Metals are also emitted from various exhaust-related sources such as fuel and lubricant combustion, particulate filters, engine corrosion, automotive coatings elements corrosion, or catalytic converters (Sýkorová et al., 2012). According to Hong et al. (2018) vehicle exhaust still should be considered as a potential main contributor to Pb pollution on urban road surfaces.

In general, several approaches and statistical methods are used for tracking the HM sources in the urban ecosystem – just to mention a few, principal component analysis (PCA) (Wang et al., 2015) and positive matrix factorisation (PMF) (González-Macías et al., 2014), which reduce a set of the raw data into principal components suggesting the contamination sources. These methods could underestimate the number of sources by not including the entire raw dataset (Hong et al., 2018). Therefore, to support the considerations of possible HM sources,

other approaches should be used. Recently Hong et al. (2018) applied a flag element ratio technique, which is widely used for groundwater studies, to track HM pollution on urban roads. The flag element ratio method does not require complex parameters and mathematical calculations; therefore, its extension to other fields is relatively easy (Hong et al., 2018). Recently, a powerful tool for studying the fingerprint of Pb sources relies on Pb isotopic composition determination (Zaborska, 2014). In general, Pb has four stable isotopes: ^{204}Pb, ^{206}Pb, ^{207}Pb, and ^{208}Pb. The variation of isotopic ratios is used as an indicator of Pb contamination in the environment (fingerprint of the Pb sources). Deduction concerning the isotope ratios is based on the different half-lives of the ^{206}Pb, ^{207}Pb, and ^{208}Pb parent isotopes. The Pb source can have diverse or overlapping isotopic ratio ranges based on which the origin of the pollution can be verified. In environmental sciences ^{206}Pb/^{207}Pb, ^{208}Pb/^{206}Pb, and ^{207}Pb/^{208}Pb ratios are commonly used. According to Sun et al. (2018), the anthropogenic sources of Pb have relatively low ^{206}Pb/^{207}Pb ratios in the ranges from 0.96 to 1.20, while naturally occurring Pb has generally higher ^{206}Pb/^{207}Pb ratios (>1.20). Zaborska (2014) reported the ratio of ^{206}Pb/^{207}Pb equal to 1.22 as a representative for old and uncontaminated Polish rocks. The ratio of ^{206}Pb/^{207}Pb in leaded gasoline used in Central and Eastern Europe was 1.16–1.17, while in unleaded gasoline and diesel fell within the ranges 1.14–1.15 and 1.14–1.16, respectively (Yao et al., 2015). Chrastný et al. (2018) reported the ^{206}Pb/^{207}Pb and ^{208}Pb/^{206}Pb ratios in unleaded gasoline and diesel from Russia equal to 1.10 and 2.06, respectively. In European coal ^{206}Pb/^{207}Pb is in the range from 1.17 to 1.19 (Komárek et al., 2008). The ^{208}Pb/^{206}Pb ratios below 2.08 are characteristic for natural/coal source of Pb, while ratios above 2.08 indicate the contribution of gasoline Pb (Zaborska and Zawierucha, 2016).

In the HM analyses of environmental samples, an important aspect which should be considered is the harmful effect of HM on human health and ecosystems. HMs are absorbed by the human body through three pathways such as inhalation, ingestion, and dermal absorption (Hu et al., 2012). Some metals are essential to life and play vital roles as a source of vitamins and minerals in the functioning of the organism, though most of them become toxic at higher concentrations (Kamunda et al., 2016). For instance, Pb is the second hazard on the priority list of HM pollutants as designated by the ATSDR (United States Agency for Toxic Substances and Disease Registry, 2007) since it is regarded as a human mutagen and probable carcinogen. Cadmium is known to be toxic even at low concentrations, while the Cr(VI) is known to be mutagenic and carcinogenic. Therefore, human contact with road dust, road particles, diverse types of car waste could increase certain risks, including carcinogenic contamination (Kamunda et al., 2016; Zhao et al., 2014).

To control and eliminate the pollution from the traffic system more effectively, information on the sources and distribution of HM in road waste is necessary. Moreover, the establishment of possible pathways of HM sources caused by car systems could be controlled where they formulate (e.g. car mechanics, vehicle diagnostic stations). The combination of different source tracking methods allows for more accurate typing of sources. The main research issue which we consider in this paper is the connection between bottom sediments of retention tanks located on urban streams and road sweeping wastes that migrate during surface runoff to the stormwater drainage systems with discharge to the retention tanks. Moreover, we focus on the primary sources of HMs in road sweeping wastes by analysing the mechanical wastes produced by vehicles. The specific research aims are as follows: 1) comparison of the level of HM contamination in bottom sediments and road sweeping waste (RSW), 2) assessment of the risk of HM contamination from vehicle traffic with an analysis of mechanical waste (MW) samples collected from four stages at a vehicle test centre and vulcanisation workshop, 3) application of PCA, Pb isotope ratio as well as the flag element ratio approach to track the sources of HM and indicate which car parts contribute to the target environment pollution by the analysed HM, 4) establishment of the human health risk related to contact via various pathways (dermal, ingestion, inhalation) with RSW and MW.

2. Methodology

2.1. Sampling area

Our research was performed in Gdansk in northern Poland (Central Europe). Gdansk has characteristics that are distinctive to a typical urban environment, which manages the largest seaport in Poland. This classification is determined by the dense population (over 460,000 residents per 262 km^2), a relatively high level of productivity driven by non-agricultural activities, infrastructure, dense road networks, buildings, and an extensive motor transportation network (Badach et al., 2020). The stormwater sewer system in Gdansk contributes to numerous urban streams outflowing to the Gulf of Gdansk (Baltic Sea). Due to the high altitude diversity of the city area, the streams have quite large slopes (similar to mountain streams), which required flood protection in the form of an expanded retention tank system. Herein the solids material transported by streams, discharged by drainage system as well as originating from surface runoff is deposited.

The average annual temperature in Gdansk is 6.8 °C with the lowest temperature reported in January–February (−4.5 °C) and the highest in July–August (20.2 °C) (average from 30 years 1982–2012; https://pl. climate-data.org/, n.d.). Throughout the year there are 162 rainfall days, and 507.3 mm of precipitation is accumulated. Most precipitation falls in July and the least in February. Due to the sea impact and climate change the episodes with temperature < 0 °C are becoming rarer (Kundzewicz et al., 2018).

2.1.1. Sediments

The bottom sediments of two retention tanks (RT) connected with the stormwater drainage system in Gdansk were collected during three seasons in 2017 – spring S—I (March–May), summer S-II (June–August), and autumn S-III (October–November). For the presented research, two main urban streams in Gdansk were chosen – Strzyza Stream with the Potokowa RT and Oliwski Stream with the Grunwaldzka RT (Fig. 1). The samples were collected and processed according to the procedure described by Nawrot et al. (2019) and Wojciechowska et al. (2019).

2.1.2. Road sweeping waste

Two main intersections in Wrzeszcz (close to Potokowa street) and Oliwa (close to Grunwaldzka avenue) city districts were selected to collect the RSW from road surfaces next to the gully tops (GT). The location of the sampling points in Potokowa-Slowackiego and Grunwaldzka intersections is presented in Fig. 1. The RSW sampling points were selected based on the stormwater drainage system network, close to the gully tops with the direct connection with the channel with stormwater discharge to the analysed retention tank. The coordinates of the sampling points are as follows: GT POTOKOWA (GT P): 54°22′25.5″N 18°34′06.5″E, GT SLOWACKIEGO (GT S): 54°22′28.0″N 18°34′06.2″E, GT1 GRUNWALDZKA (GT G1): 54°24′40.6″N 18°34′00.5″E, and GT2 GRUNWALDZKA (GT G2): 54°24′43.1″N 18°33′59.2″E.

The RSW samples were collected during three sampling campaigns which corresponded with the sediment sampling seasons. The RSW sampling campaigns took place during rainless days after at least 3 rainless days before the measuring campaign. The RSW composite samples were collected from 3×1 m^2 plots next to the gully tops (before, behind, and next to) as presented in Fig. S.1. The road surfaces were swept in dry conditions and collected into PE bags. The RSW were transported to the laboratory and dried to a constant weight using a lyophilizer.

2.1.3. Mechanical waste

The MW samples were collected from four stages at the vehicle test centre (diagnostic station) and vulcanisation workshop in four campaign replications. The subsequent positions include mechanical waste from vulcanisation (V), tyre balancer (TB), tyre scraps (TS), and wheel alignment system for cars (WA) (Fig. S.2).

The technical parameters at the mechanical complex are as follows:

a) number of vehicles serviced at the diagnostic station: 300 vehicles per month;
b) number of tyres exchanged in the winter season (October–December): 4500 pieces, in summer season (March–May): 3500 pieces;
c) weight load of vehicle diagnostic station: 40 tons, vulcanisation: 4.5 tons.

2.2. Laboratory testing

Sediments, RSW (from four locations: GT P, GT S, GT G1, and GT G2) and MW (from four stages: V, TB, TS, WA) were tested for zinc (Zn), copper (Cu), lead (Pb), cadmium (Cd), chromium (Cr), nickel (Ni), and iron (Fe).

2.2.1. Sediments

The sediment samples were initially digested using mixed acids $HClO_4$, HF, and HCl (3:2:1; Suprapur) according to the method described by Nawrot et al. (2019). Dilutions of ×10, ×100, and ×1000 were prepared. The solutions were analysed for Zn, Cu, Pb, Cr, and Ni with a flame atomic absorption spectrometer (AAS) and Cd by inductively coupled plasma mass spectrometry (ICP-MS). The results are presented in mg/kg d.w. The measurements were carried out in three replications. Quality control was assured by analysing certified reference sediments (IAEA-433 and JMS-1 and "blanks", according to the same procedure). Recoveries in the range of 92–103%, depending on individual metals, were achieved, thus indicating good agreement between certificated and analytical values. The precision, given as Relative Standard Deviation, was in the range of 3–5%. The detection limits (LOD) of each element was calculated as Blank +3·SD, where the SD values were the standard deviations of the blank samples ($n = 5$). LODs were as follows: Zn = 0.5 mg/kg d.w., Cu = 0.3 mg/kg d.w., Pb = 1.0 mg/kg d.w., Cr = 1.5 mg/kg d.w., Ni = 0.7 mg/kg d.w., Cd = 35 mg/kg d.w..

2.2.2. Road sweeping waste and mechanical waste

The mineralization procedure for 0.2 g of RSW (GT P, GT S, GT G1, and GT G2) and MW (V, TB, TS, WA) ashes (after 8 h of combustion of dried sediments in 450 °C in the muffle furnace) was performed using microwave digestion with the use of 2 cm^3 HNO_3, 1 cm^3 $HClO_4$, and 3 cm^3 of HF (Extrapure). The microwave oven Berghof "speedwave" was used (Fig. S.3). The mineralization process was performed in steps using the following parameter: 170 °C for 8 min (35 bar, slope 2 min, power 70%), 220 °C for 20 min (35 bar, slope 3 min, power 90%), 50 °C for 10 min (25 bar, slope 1 min, power 0%), 100 °C for 1 min (20 bar, slope 1 min, power 10%), and 100 °C for 1 min (20 bar, slope 1 min, power 10%). These microwave mineralization parameters are a combination of the application note from Berghof.com for "Berghof speedwave" for microwave mineralization for ashes and caoutchouc. After the acids were evaporated to dryness and the samples were taken out of the rotor body, 10 ml of water (Milli-Q) was added and the samples were transferred to 50 ml volumetric flasks and filled to a volume of 20 ml. The samples were stored in cooling conditions (8 °C) until the analysis with ICP-MS.

Lead stable isotopic ratios were measured in a Perkin–Elmer Sciex ELAN 9000 ICP-MS. The international NBS-981 standard was measured to indicate that our results were within the certified values and in agreement with the long-term internal laboratory reproducibility. The results of this study were satisfactory and the recovery was >95%. The repeated digestion and analysis of NBS-981 ($n = 5$) were performed together with all samples set. The mean $^{207}Pb/^{206}Pb$ was 0.94834 ± 0.00289 (certified value = 0.91464) and the mean $^{208}Pb/^{206}Pb$ was 2.17449 ±
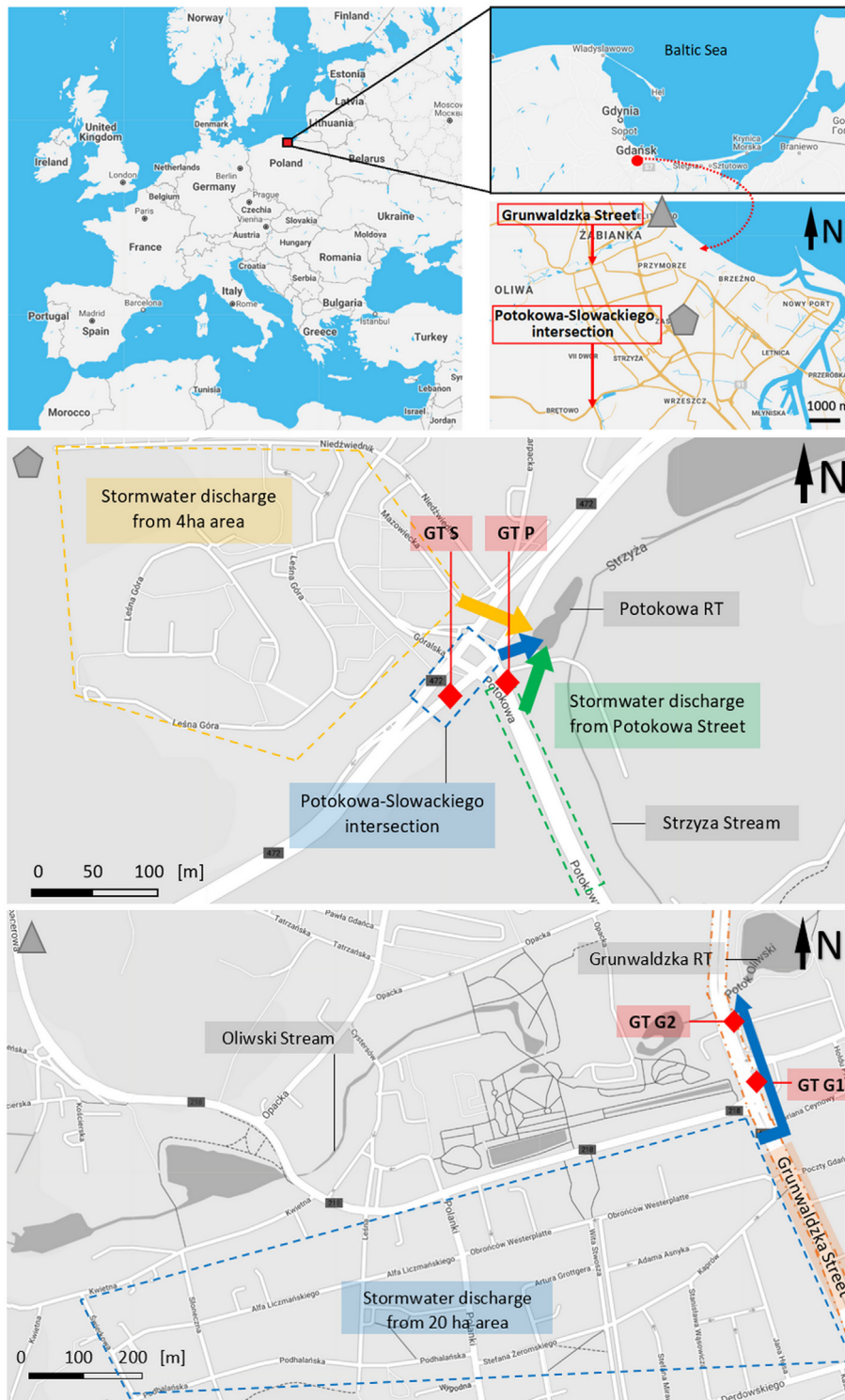
Fig. 1. The location of the gully tops in Potokowa-Slowackiego intersection and Grunwaldzka Street. GT P, GT S, GT G1, and GT G2 – gully tops plots; RT – retention tank.

0.00702 (certified value = 2.16810). Three blank samples (containing only chemicals) were measured with every ten samples. The detection limits (LOD) of every element was calculated as Blank $+ 3 \cdot$ SD, where SD was standard deviations of the blank samples (measured ten times). The blank samples were prepared from Suprapur 0.1 M HNO$_3$. LODs as follows: ^{206}Pb = 0.007 µg/dm^3, ^{207}Pb = 0.007 µg/dm^3, and ^{208}Pb = 0.007 µg/dm^3. Mean RSD was calculated from triple analysis (separate digestion and measurement of 3 parallel subsamples) of

every third sample. It was equal to 0.17% for ^{206}Pb/^{207}Pb ratio and 0.53% for ^{208}Pb/^{206}Pb ratio.

2.3. Contamination status and risk assessment

The assessment of HM contamination was performed using the contamination factor CF (Chabukdhara and Nema, 2013; Tomlinson et al., 2013) according to formula (1):

$$CF = \frac{C_{mSample}}{C_{mBackground}} \tag{1}$$

where $C_{mSample}$ is a HM concentration in the analysed sample and $C_{mBackground}$ is the geochemical background concentration. The $C_{mBackground}$ value established for urban sediments in retention tanks in Gdansk by Wojciechowska et al. (2019), on the basis of classification provided by Kowalska et al. (2018) is presented in Table S.1. Four contamination categories of CF are distinguished by Hakanson (1980): CF < 1: low contamination, 1 ≤ CF < 3: moderate contamination, 3 ≤ CF < 6: considerable and CF ≥ 6: very high contamination.

The ecological risk assessment was carried out with the use of potential ecological risk (RI) (Mandeng et al., 2019) according to formula (2):

$$RI = TR \cdot CF \tag{2}$$

where TR is the toxic response factor suggested by Hakanson (1980). TR suggested for Cr, Ni, Cu, Cd, Pb, and Zn are 2, 6, 5, 30, 5, and 1, respectively. Four risk levels are described: RI < 150: low ecological risk, 150 ≤ RI < 300: moderate ecological risk, 300 ≤ RI < 600: significant ecological risk, RI ≥ 600: high ecological risk.

2.4. Human health risk assessment

2.4.1. Non-carcinogenic and carcinogenic assessment via ingestion, dermal contact, and inhalation

Non-carcinogenic and carcinogenic risk assessment in the present study was calculated with the method described by US EPA (1989) based upon consideration of human exposure to RSW and MW via three different pathways including ingestion ($_{ing}$), dermal contact ($_{dermal}$), and inhalation ($_{inh}$). The exposure scenario included lifelong, chronic exposure of adults and children to Zn, Cu, Cd, Pb, Ni, and Cr. It was assumed that the entry of HM into the body occurs unintentionally. The *Intake* ($mg \cdot kg^{-1} \cdot d^{-1}$) is introduced for non-carcinogenic elements, comprising Cu, Pb, and Zn and the mean lifetime average daily dose (hereafter called LADD, $mg \cdot kg^{-1} \cdot d^{-1}$) is adopted for carcinogenic elements, inclusive of Cr, Ni, and Cd. The intake estimations via each exposure pathways (*Intake*/or *LADD* in cancer risk calculations) were calculated using the following formulas (3)–(5):

$$Intake\ (LADD)_{ing} = C_m \cdot \frac{IngR \cdot EF \cdot ED}{BW \cdot AT} \cdot 10^{-6} \tag{3}$$

$$Intake\ (LADD)_{dermal} = C_m \cdot \frac{SA \cdot SAF \cdot ABF \cdot EF \cdot ED}{BW \cdot AT} \cdot 10^{-6} \tag{4}$$

$$Intake(LADD)_{inh} = C_m \cdot \frac{InhR \cdot EF \cdot ED}{PEF \cdot BW \cdot AT} \tag{5}$$

where C_m is the mean HM concentration in the analysed sample [mg/kg d.w.] and 10^{-6} is the unit conversion factor: $10^{-6} kg \cdot mg^{-1}$ (US EPA, 2001). Other factors and their values used for calculations are presented in Table S.2.

The hazard quotient HQ to assess the non-carcinogenic toxic risk was determined as follows (US EPA, 1989):

$$HQ = \frac{Intake}{RfD} \tag{6}$$

where *Intake* is the doses absorbed via 3 different pathways and *RfD* is the reference dose, which is an estimate of the daily exposure to the human population (including sensitive subgroups) that is likely not to pose an appreciable risk of deleterious effects during a lifetime. The *RfD* values were established based on the toxicology data base (IRIS Assessment by USEPA) as well as with reference to Qing et al. (2015) and Wei et al. (2015).

The chronic hazard index HI, which is the sum of more than one HQ for multiple substances or multiple exposure pathways, can be calculated from:

$$HI = \frac{Intake_k}{RfD_k} \tag{7}$$

where the $Intake_k$ is the daily intake of the HM k and RfD_k is the chronic reference dose for the HM k. Based on the US EPA recommendation, the possibility of negative health effects occurs when HI > 1, while when HI ≤ 1 adverse health effects are unlikely to appear.

The Incremental Lifetime Cancer Risk ILCR used to calculate the carcinogenic risk is presented in Eq. (8):

$$ILCR = LADD \cdot SF \tag{8}$$

where *LADD* is the chronic daily intake of carcinogens ($mg \cdot kg^{-1} \cdot d^{-1}$) and *SF* is the slope factor of hazardous substances ($kg \cdot mg^{-1} \cdot d^{-1}$).

The cumulative cancer risk (Eq. (9)) is the sum of individual *ILCR* for analysed elements and can be calculated from:

$$Total\ cancer\ risk = LADD_k \cdot SF_k \tag{9}$$

where $LADD_k$ is the chronic daily intake ($mg \cdot kg^{-1} \cdot d^{-1}$) of HM k, and SF_k is the slope factor for HM k ($kg \cdot mg^{-1} \cdot d^{-1}$). The acceptable or tolerable risk for regulatory purposes is within the range of 10^{-6}–10^{-4} (US EPA, 2001). The value of *Totalcancerrisk* greater than 10^{-4} indicates the high risk of developing cancer in humans. The description of the carcinogenic class, *RfD*, and *SF* for analysed elements is presented in Table S.3.
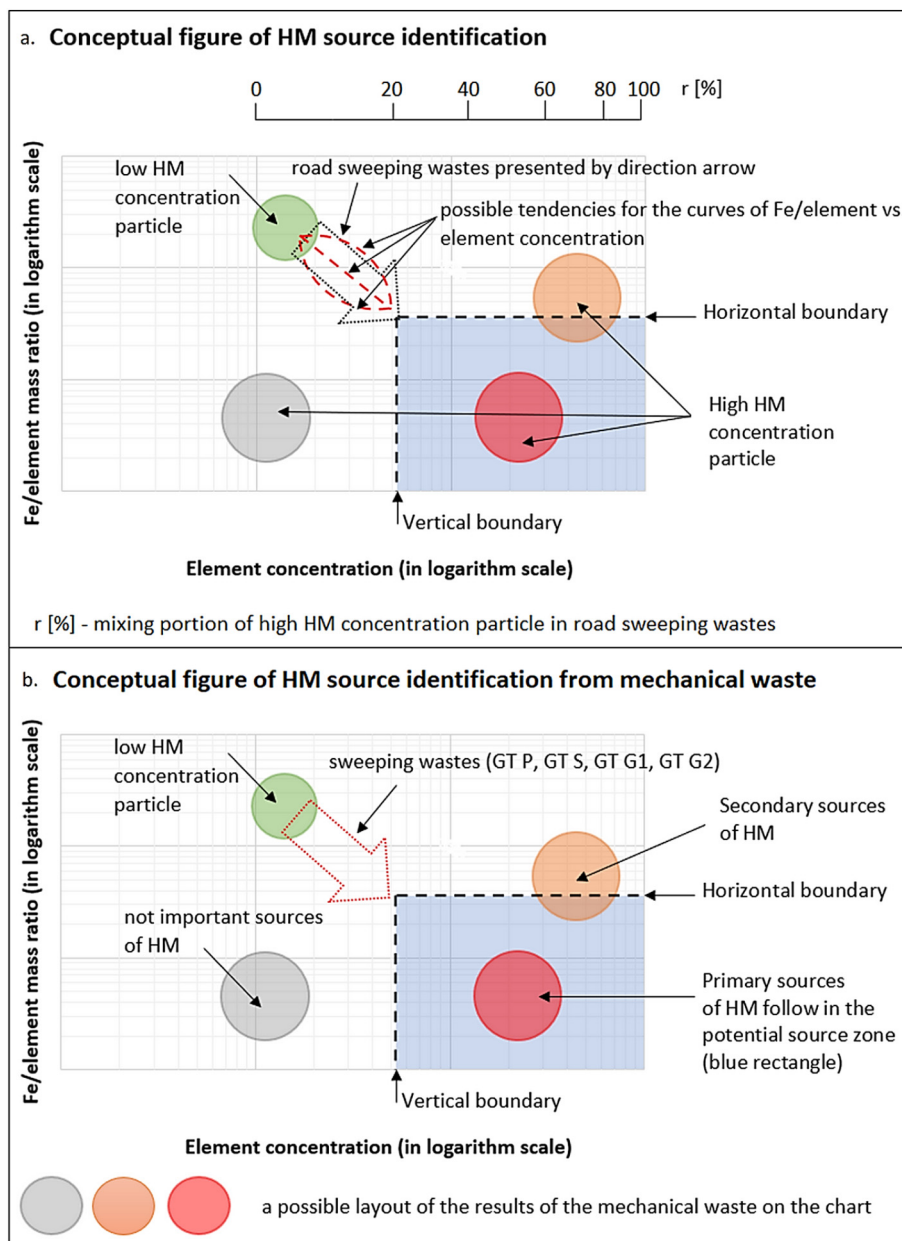
2.5. Source tracking approach

2.5.1. Statistical analysis using PCA and correlations

Correlations of metal elements in sediments collected from retention tanks RSW and MW were calculated using the nonparametric Spearman rank method. Ward's cluster analysis (CA) and principal component analysis (PCA) were carried out for measuring HM in solid samples. In the PCA, the number of principal components was determined on the basis of Cattell's test. PCA is a mathematical procedure that uses an orthogonal transformation to convert a set of observations of possibly correlated variables into a set of values of linearly uncorrelated variables (Zhao et al., 2014). The result is a rotated component matrix for PCA loadings. The data analysis was performed using Statistica® 13.1 software.

2.5.2. Flag element ratio and Pb isotopes

To track sources of HM pollution on urban roads the flag element ratio approach recently developed by Hong et al. (2018) was used (Fig. 2). This approach applies the flag element usually with a higher amount than other elements that are targeted for source tracking in the natural environment. As a flag element, iron (Fe) was used (in our study Fe loads were by two or three orders of magnitude higher than the analysed HM). The general conception of source identification for HM (Fig. 2a), developed by Hong et al. (2018) based on the curves of Fe-HM ratio versus HM concentration on a logarithmic scale, distinguished the potential source zone (blue rectangle) – i.e. the primary source. The direction arrow which shows the possible tendencies for the curves of Fe-HM ratio versus HM concentration is indicated by the particles from the low to high HM concentrations. The potential source zone is formed by the horizontal and vertical boundaries and the point of the direction arrow. The inference from the conceptual figure of the source identification for HM relies on the assessment of the degree of the overlapped area between the particle distribution area (on the chart) and the potential source zone. The criteria to rank sources are

Fig. 2. The conceptual figure of source identification for heavy metals (HMs) using the Fe/HM ratio approach based on Hong et al. (2018); a) general conception, b) the interpretation of the tracking source approach for road sweeping and mechanical wastes.

as follows: particles with a distribution area completely falling into the potential source zone (namely the area of the red direction pointing arrow, cf. the red circle in Fig. 2) are considered as the primary HM sources. The sources partly falling into the blue square area (cf. the orange circle in Fig. 2) were considered as the secondary HM sources, while the sources not falling into the blue square area (cf. the grey circle in Fig. 2) are considered as insignificant HM sources. The interpretation of the tracking source basing on the flag element ratio for RSW and MW is presented in Fig. 2b (the results for RSW follow with the direction arrow, while the possible position of MW results is presented by circles).

For distinguishing between separate Pb sources, a three-isotope plot ($^{206}Pb/^{207}Pb$ vs. $^{208}Pb/^{206}Pb$ vs. $^{208}Pb/^{207}Pb$) was applied. These approaches allow for more precise identification of separate Pb sources.

3. Results & discussion

3.1. Heavy metal concentrations and contamination of sediments and waste sources

3.1.1. Bottom sediments

The average HM concentrations in bottom sediments of the retention tanks – Potokowa and Grunwaldzka – for the 3 analysed seasons are presented in Fig. 3. Zn featured the greatest variability of concentration during the spring (S—I), summer (S-II), and autumn (S-III) seasons. The seasonal changes were between 200 mg/kg d.w. (S—I) to almost 600 mg/kg d.w. (S-II) in Potokowa, while for Grunwaldzka they ranged from 87.5 mg/kg d.w. (S-II) to 200 mg/kg d.w. Seasonal variability also affected Cu and Cd concentrations in Potokowa as well as Pb concentration in Grunwaldzka. For other elements, the concentrations remained
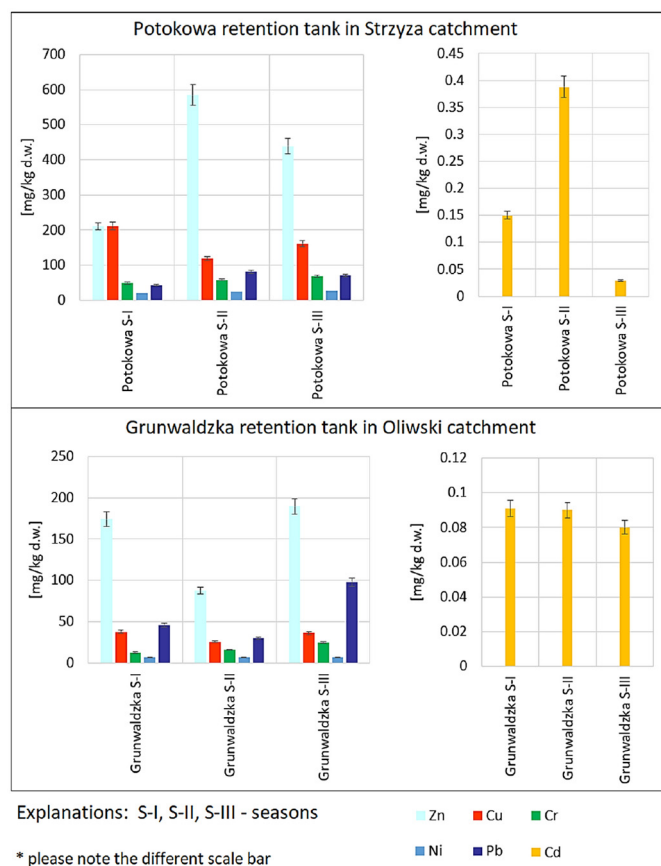
Fig. 3. The average HMs concentration [mg/kg d.w.] in sediments deposited in Potokowa and Grunwaldzka during the three analysed seasons.

stable during all seasons. During the S—I, in which the average 3-month precipitation height was the lowest (97 mm) compared to S-II (198 mm) and S-III (148 mm), the increase of HM content in sediments in relation to the precipitation height was visible only for Zn, Cd, and Ni in Grunwaldzka. Islam et al. (2015a, 2015b) confirm the differences of HM content in bottom sediments for winter and summer seasons. In their study, in general, HM contents (concerning Cu, Pb, Cd, Ni, and Cr) were higher in the winter season. Previous studies provided by Sakson et al. (2018) on the urban catchment in Łódź (Poland) prove that stormwater discharge caused a high emission of Cu and Zn. The CF and RI values are presented in Table 1. The CF in Potokowa indicated considerable contamination status for Ni, Pb (all seasons), and Zn (S—I,). Very high contamination according to CF was observed for Cu, Cr (all seasons), and Zn (S-II and S-III). A moderate ecological risk was observed for Cu in S—I and S-III. Sediments deposited in Grunwaldzka were at the top end of the moderate contamination status. HM content in sediments of the river flowing through the urban gradient in Eastern China was reported by Wu et al. (2017) at a following mean level [mg/kg d.w.]: 149 for Zn, 44.7 for Cu, 33.4 for Pb, 0.61 for Cd, 34.6 for Ni, and 79.9 for Cr. A similar HM content was described by Unda-Calvo et al. (2019) for Deba River sediments (Spain) in an urban catchment area. These results are in line with those obtained for Grunwaldzka, except Cd. The investigation performed by Zemełka et al. (2019) for the Dobczyce reservoir (a drinking water reservoir in Poland) and its tributaries shows significantly lower Zn, Pb, and Cu content in its bottom sediments. However, in the case of suspended sediments for tributaries flowing mainly through agricultural land, elevated values of Zn (385 mg/kg d.w.) and Cd (0.462 mg/kg d.w.) was reported. Therefore, it was expected that atmospheric precipitation could by threatened by emissions from the relatively distanced urban and industrial agglomeration of Cracow. HM content in sediments serves as an indicator of the

pollution level and screening tool to fingerprint the historical and/or recent contamination in the surrounding environment (Hanif et al., 2016).

3.1.2. Road sweeping and mechanical waste

Characteristic concentrations of HM in RSW and MW are shown in Table 2. The concentrations of all analysed HM were higher for waste collected from vehicle diagnostic station. The greatest mean observed values were as follows [mg/kg d.w.]: 8444 for Zn (WA), 3308 for Cu (WA), 291 for Pb (V), 2.81 for Cd (TS), 154 for Ni (V), and 550 for Cr (WA). The mean concentration of HM for V followed a descending order as Zn > Cu > Cr > Pb > Ni > Cd, for TB Zn > Pb > Cu > Cr > Ni > Cd, for TS Zn > Cu > Pb > Ni > Cr > Cd, for WA Zn > Cu > Cr > Ni > Pb > Cd, which means that Zn, Cu, and Pb have the significant share in the MW from vehicle diagnostic station. HM content in RSW collected near the gully tops was significantly lower than observed for MW from vehicle centre. The max reported values were in the ranges [mg/kg d.w.] from 82.5 (GT P) to 111 (GT G1) for Zn, from 63.9 (GT P) to 106 (GT S) for Cu, from 24.5 (GT G1) to 36.8 (GT G2) for Pb, from 0.057 (GT G1) to 0.425 (GT G2) for Cd, from 8.45 (GT G1) to 16.9 (GT S) for Ni, and from 31.2 (GT G1) to 111 (GT G2) for Cr. In general, the highest HM content for RSW was reported for the GT located on Grunwaldzka Street (with regard to Zn, Pb, Cd, and Cr). According to traffic volume measurements, Grunwaldzka experiences approx. 58,929 vehicles per day. In relation to the Walpurgisstr. site (which is a main road in Dresden with an average daily traffic of 12,600 vehicle per day) reported by Zhang et al. (2017) the obtained results in our study were 4–11 times lower for Zn, 1.5–3 times lower for Cu, and were similar in the case of Cd. According to the literature, the main sources of HM supplemented by traffic consist of brake and tyre wear, motor oil and traffic for Zn, brake wear, stop points, traffic for Cu, brake, oil and additives, gasoline, and traffic for Pb, tyre wear for Cd, brake wear and traffic for Ni, as well as brake and tyre wear with traffic for Cr (Ferreira et al., 2016). Metals that deserve special attention in our study are Cr (due to the high content reported for GT G2) and Cu (due to the high content reported for GT S and GT G1).

The analysis of MW from the vehicle diagnostic station indicates some possible ecological impacts. In the case of Zn, the highest value was reported in TS. Tyres contain a vast range of organic and inorganic constituents, although many of them are not exclusively specific for tyres and can stem from other sources. The high concentrations of Zn in tyres result from the addition of ZnO and ZnS during vulcanisation. The percentage range of Zn in tyres changes from 0.4% to 4.3% (Adamiec et al., 2016). Hong et al. (2018) noted a mean 10,000 mg/kg Zn concentration in tyre scraps samples. A concentration of Zn almost 2.5 times lower (in comparison to TS) was observed in waste collected from WA. At this stage, apart from the vehicle correcting wheel alignment, a machine is used for checking the suspension vibration damping efficiency. In all probability, data similar to WA could be observed during extreme vehicle operation – e.g. car racing or car accidents. In the V stage, the Zn concentration was 2 times lower than observed for WA, while the Zn content share in TB waste was at a moderate level. Conterminous results were observed for WA and V due to Cu, Ni, and Cr content. The Pb concentration was the highest for V and TB waste, which means this metal was inputted as a result of using drive system actuators. Elevated Cd concentration was observed for TS (in relation to all analysed MW), which coincide with the tyre wear source reported in the literature (Ferreira et al., 2016; Hong et al., 2018). The results observed for WA were in line with Zn, Cu, Pb, Ni, and Cr concentrations described by Hong et al. (2018) for wear particles collected from waste brake shoes.

3.2. Health risk assessment of road sweeping waste and mechanical waste

The assessment of non-carcinogenic and carcinogenic risk due to HM exposures in MW from vehicle diagnostic station and RSW from road intersections are shown in Figs. 4 and 5. The maximum HQ value via ingestion, inhalation, and dermal contact was observed for Cr for

Table 1
The assessment of contamination factor (CF) and potential ecological risk (RI) for sediments deposited in Potokowa and Grunwaldzka during the three analysed seasons.

Index	Metal	Bottom sediments from retention tanks					
		Strzyza catchment			Oliwski catchment		
		Potokowa S-I	Potokowa S-II	Potokowa S-III	Grunwaldzka S-I	Grunwaldzka S-II	Grunwaldzka S-III
Contamination Factor CF	Zn	**4.7**	**13**	**9.8**	1.4	0.7	1.6
	Cu	**50.4**	**28.4**	**38.4**	2.2	1.5	2.2
	Cr	**10.4**	**12.5**	**14.5**	1.4	1.8	2.8
	Ni	**3.8**	**4.6**	**4.7**	1.3	1.3	1.2
	Pb	2.6	**4.9**	**4.3**	1.2	0.8	2.5
	Cd	0.6	1.6	0.1	0.1	0.1	0.1
Potential ecological risk RI	Zn	5	13	10	1	1	2
	Cu	**252**	142	**192**	11	8	11
	Cr	21	25	29	3	6	6
	Ni	23	27	28	8	7	7
	Pb	13	25	21	6	13	13
	Cd	18	47	3	3	3	3

Bold: CF - higher than considerable contamination status of sediments; RI – sediments with moderate ecological risk.

WA among MW and GT G2 among RSW (for adults and children). It was indicated that the exposure pathways of the metals for both adults and children ran in the following descending order: ingestion > dermal contact > inhalation. For all elements, the contribution of HQ_{ing} to HI were the highest – from 83.3% to 99.1% for adults and from 98.5% to 99.9% for children. These percentage shares suggest that ingestion was the main exposure pathway that might threaten human health. Similar results were observed by Chabukdhara and Nema (2013) and Qing et al. (2015). In general, the MW samples from the vehicle diagnostic station present higher values of health risk than RSW.

The highest non-carcinogenic risk in MW observed for V was caused by Cr and Pb, for TB by Pb and Cr, for TS by Zn and Pb, and for WA by Cr and Cu. The HI indicated possible negative health effects for children for V (Cr, Pb) and WA (Cr, Cu). For RSW the highest HI was observed for GT G2, although it was lower than unity. The total carcinogenic risk raises concerns due to the Cr content in all waste samples. The health risk for children should receive attention due to the pica behaviour and hand or finger sucking which could cause the ingestion of significant quantities of solid material or dust (Zhao et al., 2014). HM occurrence could be especially detrimental to the children's health due to the weakness of their immune system (Yang et al., 2011). Several studies (Chabukdhara and Nema, 2013; Qing et al., 2015) focused on soil or sediment health risk assessment confirm that urban and industrial solid material did not pose a carcinogenic risk from Ni, Cd, and Cr. However, Cr pollution should not be ignored in terms of children's or adults' health. Children face more health risk in their daily life than adults and their contact with potentially toxic materials should be restricted.

The exposure frequency applied in the calculations was 350 days/year, which together with the exposure duration time (30 years for adults and 6 years for children) shows that the presented non-carcinogenic and carcinogenic risk is overstated. It is worth noting here that not all of these hazardous substances could infiltrate urban dust (and penetrate the human body in this form). Workers in the diagnostic vehicle station as well as in the mechanic car repair shops are in
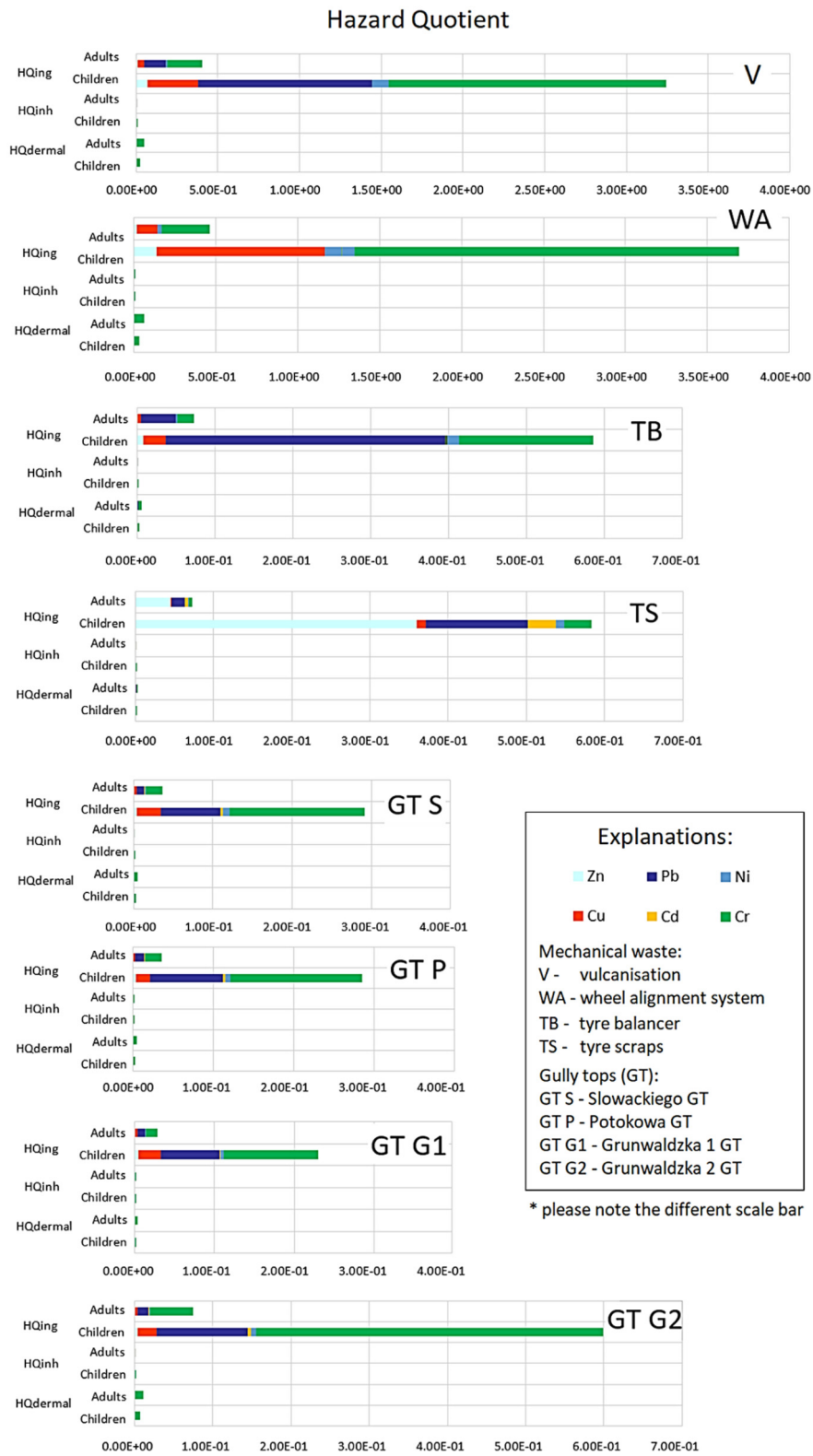
Table 2
HM concentrations [mg/kg d.w.] in road sweeping waste (RSW) collected near the gully tops and in mechanical waste (MW) collected from different stages in vehicle diagnostic station: vulcanisation – V, tyre balancer – TB, tyre scraps – TS, wheel alignment system for cars – WA.

Element	Value	MW				RSW			
		V	TB	TS	WA	GT S	GT P	GT G1	GT G2
Zn	min	1459	154	6989	2987	64.1	52.1	92.5	87.9
	max	1785	210	10,477	3603	88.2	82.5	111	99.0
	mean	**1659**	179	**8444**	**3308**	76.5	67.3	**103**	94.2
	median	1697	175	8155	3322	76.2	68.9	104	94.9
Cu	min	812	87.5	31.2	2974	81.4	45.2	82.1	66.3
	max	1082	105	45.6	3512	106	63.9	95.2	85.6
	mean	**961**	92.9	37.4	**3210**	**95.0**	55.2	87.2	75.4
	median	975	89.5	36.4	3178	94.5	53.2	86.2	73.2
Pb	min	201	87.8	32.3	22.5	18.2	21.5	17.8	28.9
	max	412	112	42.5	29.7	22.6	28.2	24.5	36.8
	mean	**291**	**97.8**	35.7	26.4	20.7	24.9	20.3	**31.8**
	median	276	95.5	34.0	26.7	20.6	24.4	19.8	30.9
Cd	min	0.090	0.298	2.12	0.388	0.187	0.185	0.041	0.312
	max	0.222	0.355	3.35	0.412	0.327	0.245	0.057	0.425
	mean	0.160	0.327	**2.81**	0.398	0.228	0.218	0.049	**0.366**
	median	0.165	0.328	2.88	0.396	0.221	0.215	0.052	0.369
Ni	min	119	18.9	12.6	118	11.9	7.99	6.98	8.36
	max	226	28.9	18.9	132	16.9	12.2	8.45	10.9
	mean	**154**	22.4	15.6	**124**	**14.3**	9.61	7.48	9.62
	median	135	21.0	15.5	123	14.0	9.25	7.21	9.69
Cr	min	325	34.5	7.98	498	35.8	32.5	22.1	98.7
	max	504	47.4	8.59	633	45.5	43.6	31.2	111
	mean	**398**	40.5	8.31	550	39.9	38.6	27.7	**104**
	median	382	40.0	8.34	534	39.8	39.8	27.9	102

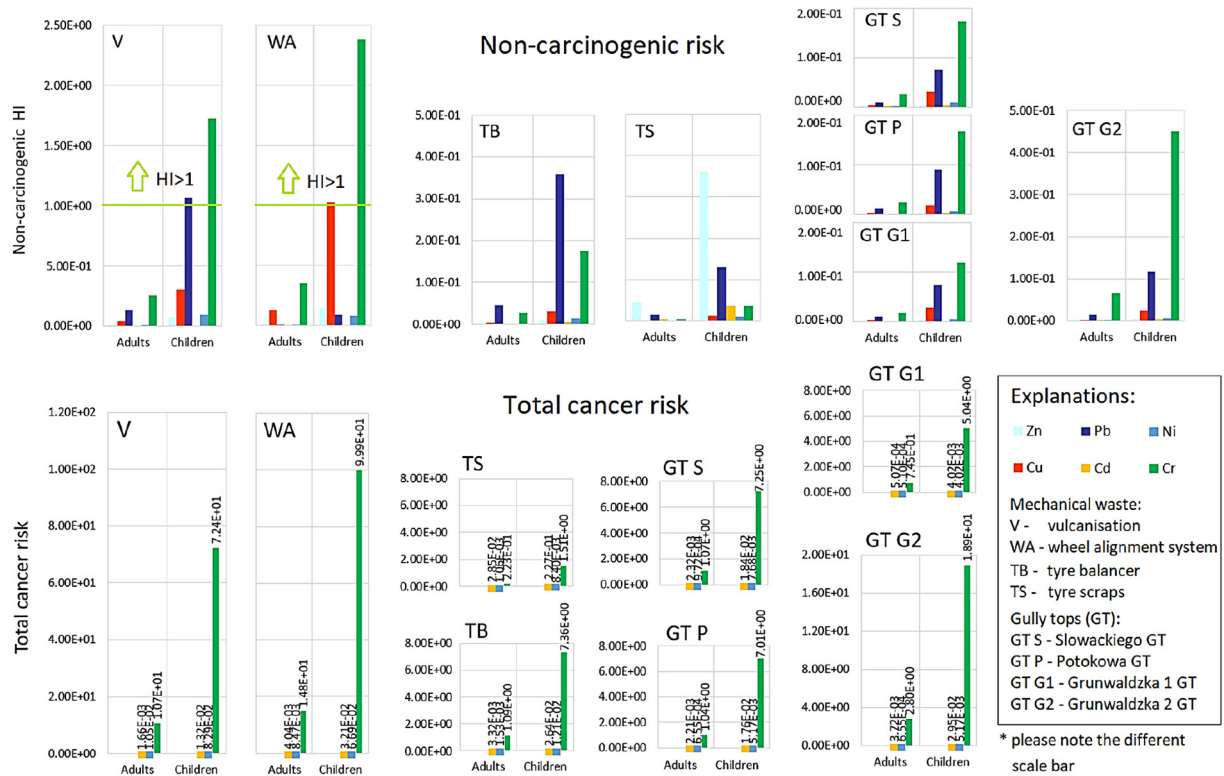**Bold:** the maximum mean observed values.

Fig. 4. Hazard quotient (HQ) of HMs in road sweeping waste (RSW) collected near the gully tops in the investigated area and mechanical waste (MW) collected in vehicle diagnostic station; ing – ingestion, inh – inhalation, dermal – dermal contact.

the high-risk exposure group. In the case of RSW the human risk is much lower, because direct contact with this kind of waste is generally excluded; in many cases pedestrian routes are located at a distance from the streets, although the transfer of contaminants to nearby green areas

(eg. residential parks) cannot be excluded. In the event of RSW entering nearby soils, for example in recreational areas, the resulting calculated health risks would be much lower due to the characteristic site exposure (EF = 75 days/year) (Luo et al., 2012).

Fig. 5. Non-carcinogenic (HI) and total cancer risk of HM in road sweeping waste (RSW) collected near the gully tops in the investigated area and mechanical waste (MW) collected in vehicle diagnostic station.

3.3. Source tracking of heavy metals

In general, the significant share of Zn, Cu, and Pb in MW coincides with the relatively high amount of these metals in RSW as well as in bottom sediments deposited in RTs, supporting the thesis of motorization as the origin of those metals. In turn, the health risk analyses pointed special attention to Cr. To elaborate on these observations we studied the relationships between metals and searched for a primary source. Our analyses were based upon several approaches including the statistical methods, Pb isotope ratios, and flag element ratio approach. The results of those methods were compared to produce final conclusions.

3.3.1. Statistical methods application

Correlations between HMs often reflect the source(s) of contamination and the dispersal of solid-associated metals within the stormwater-retention system, the latter of which is related to the redistribution of the HMs within the bottom sediments of receivers. The elements reflecting the high correlations may share common sources, similar properties during transformation and fate of migration under certain physicochemical circumstances (Wang et al., 2019). To explore the correlation analysis between seven HM concentrations in sediments and RSW collected near gully tops at two catchments, Spearman's rho matrix was employed (Table 3). For both catchments, a significant positive correlation coefficient at $P < .05$ was observed between the elemental pairs Zn—Pb (0.99 and 0.83), Ni—Cr (0.93 and 0.98), Ni—Fe (0.72 and 0.92), and Cr—Fe (0.80 and 0.91). A significant correlation was noted also for Cu—Ni (0.69 and 0.58) and Cu—Cr (0.53 and 0.56). This indicates that these elements possibly stem from the same sources, which means that supplementation of HM results from runoff from paved surfaces, where the probable origin of the contaminants is vehicle transport or fuel combustion (also caused by atmospheric deposition). Spearman's rho matrix depicted the differences between the correlation coefficient of the elements for both locations. A distinction was

observed between the elemental pairs Zn—Ni, Zn—Cr, Zn—Fe, Pb—Ni, Pb—Cr, Pb—Fe, for which a significant positive correlation coefficient at $P < .05$ was observed for RSW collected near the gully tops at the Potokowa-Slowackiego intersection and sediments deposited in Potokowa (the Strzyza Stream catchment). The correlation coefficients were as follows 0.90, 0.88, 0.79, 0.92, 0.91, and 0.81, respectively (for the elemental pairs indicated above). In the case of RSW collected at the Grunwaldzka intersections and sediments deposited in the subordinate retention tank (Grunwaldzka), an additional correlation was observed for pairs Cd—Ni (0.96), Cd—Cr (0.96), and Cd—Fe (0.98).

Table 3
Correlation analysis (Spearman's rho matrix) between analysed HM concentrations in sediment and road sweeping waste (RWS) samples collected near gully tops in the Strzyza and Oliwski catchment.

Elements							
Elements	Zn	Cu	Pb	Cd	Ni	Cr	Fe
Strzyza Stream sediments with sweeping wastes from gully tops							
Zn	1.0						
Cu	0.35	1.0					
Pb	0.99	0.41	1.0				
Cd	0.20	−0.44	0.10	1.0			
Ni	0.90	0.69	0.92	−0.10	1.0		
Cr	0.88	0.53	0.91	−0.29	0.93	1.0	
Fe	0.79	0.11	0.81	−0.18	0.72	0.80	1.0
Oliwski Stream sediments with sweeping wastes from gully tops							
Zn	1.0						
Cu	−0.42	1.0					
Pb	0.83	−0.48	1.0				
Cd	−0.37	0.36	−0.20	1.0			
Ni	−0.53	0.58	−0.39	0.96	1.0		
Cr	−0.42	0.56	−0.22	0.96	0.98	1.0	
Fe	−0.24	0.33	−0.17	0.98	0.92	0.91	1.0

The conclusions from Spearman correlation coefficients were not comprehensive, because the relationships between HMs were complex and influenced by various factors. To further examine the relationships among HMs and their source, the principal component analysis (PCA) was used. Table 4 explored the PCA loadings for HMs in sediments and RSW. The results indicated that PCA reduced the number of variables to three principal components (PCs), which explain 95.12% and 97.20% of the data variance for the Strzyza and Oliwski catchments, respectively. The first principal component (PC1) for the Strzyza catchment, loaded heavily with Zn, Pb, Ni, Cr, and Fe and slightly with Cu, accounted for 67.93% of the total variance. The Cu might imply quasi-independent behaviour within the group, which is suggested by the Cu factor loading for PC3 (−0.529) and PC1 (−0.548). The second group (PC2) accounted for 20.38% of the total variance with a high loading of Cd. The PC3 that correlated with Cu (−0.529) accounted for 4.81% of the total variance. According to Sun et al. (2019) variables with a similar loading generally have strong common correlations. Based on the factor loadings and mutual correlations, Cu could be distinguished in two groups – together with other HMs in Group 1 (Zn, Pb, Ni, Cr, Fe, *and Cu**) or separately within Group 3 (Cu). The main source of the elements gathered in Group 1 can be distinguished as traffic or coal combustion as well as mixed pathways, due to the high concentrations of these elements in sediments in relation to the background values reported for surrounding soils (Table 1). Cd and partly Cu probably originated from other sources. The Cd concentrations for sediments deposited in Potokowa and for RSW were at a level similar to the background concentration. Therefore, the Cd content in sediments and RSW could be recognised as typical for this area. Thus, Group 2 would be considered as an indicator of geochemical processes.

The PC1 for Grunwaldzka sediments and RSW for Grunwaldzka intersection was mainly loaded with Cd, Ni, Cr, and Fe and moderately loaded with Cu, which accounted for 64.97% of the total variance. Based on the considerations above and on the reference value represented by the background concentration for surrounding soils, these element concentrations slightly exceed the values reported in Table S.1. The PC2 accounted for 23.20% of the total variance with a high loading of Zn and Pb for which seasonal concentrations in bottom sediments were exceeded in relation to the background values. This means that the probable source is related to human activities, which may include

traffic. The PC3 that correlated with Cu (0.692) accounted for 9.02% of the total variance. The quasi-independent behaviour of Cu could suggest that there might be some other source of this HM. In our previous study (Nawrot and Wojciechowska, 2018), we reported that in the Oliwa district, where Grunwaldzka is located, there are many buildings with copper sheet rooftops. We also observed leaching of Cu (up to 10.23 mg/dm^{-3}) in roof runoff during wet episodes.

A cluster analysis (CA) was used to group the variables of MW collected at four stages of the vehicle diagnostic station (V, TS, TB, WA). The hierarchical clustering by applying Ward's method was performed on a standardised dataset (Cai et al., 2012). The results are presented in Fig. 6. In general, the chart presents three clusters: (1) Cd-Pb-Fe, (2) Ni-Cr-Cu, and (3) Zn. Thus, CA suggests at least three different groups of HM, although the rotated component matrix for PCA (Table 5) suggests slightly different interactions between elements which could run off into the environment via the diverse stages of the car diagnostic centre. The first group (PC1) accounted for 49.07% of the total variance with a high loading of Ni, Cd, Pb, and Cr, which means that these HM were correlated at all stages. These HM have a common source – car parts. Among PC1, the Zn loading was inversely correlated with Group 1 (−0.647). The second component (PC2) accounted for 34.65% of the total variance with a high loading of Cu (−0.845). The third component (PC3) accounted for 9.52% and it was correlated with Zn (0.638). Zinc and Cu concentrations were significantly higher in waste from vehicle diagnostic station in comparison to other elements. The highest Zn value was reported for TS. Car tyres in the EU contain nearly 1% of Zn oxide, 47% of rubber, 16.5% of metals, and 21.5% of carbon black (Pant and Harrison, 2013). Still, during car usage, a huge proportion of the Zn is emitted, as the result from V and WA suggests. Group 3 also hints that Cd behaves similarly to Zn, which is further confirmed by the results for TS (Cd mean content on the level of 2.81 mg/kg d.w.).

To sum up, the statistical analyses performed for HM concentrations detected in sediments and RSW suggests the differences in possible HMs sources:

- In Strzyza catchment traffic was depicted as the main source of (PC1) Zn, Pb, Ni, Cr, and Fe. Cd (PC2) was considered as an indicator of geochemical processes or slightly correlated with Zn (which could

Table 4
Rotated component matrix for principal component analysis loadings for HMs in sediments and road sweeping waste (RSW) samples collected near gully tops in the Strzyza and Oliwski catchments.
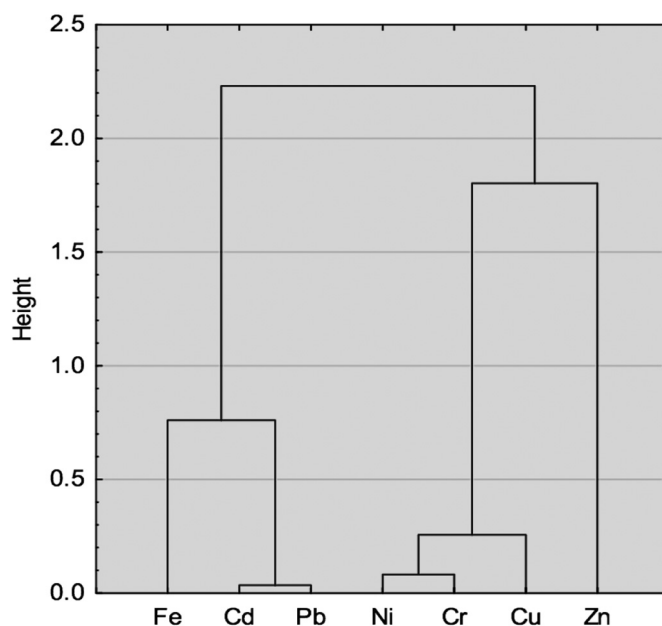
Elements	Component		
	PC1	PC2	PC3
Strzyza Stream sediments with sweeping waste from gully tops			
Zn	−0.940	0.327	−0.081
Cu	−0.548	−0.647	−0.529
Pb	−0.962	0.233	−0.063
Cd	0.131	0.900	−0.411
Ni	−0.970	−0.075	−0.206
Cr	−0.982	−0.107	0.153
Fe	−0.849	0.140	0.497
Eigenvalue	4.76	1.43	0.77
% of variance	67.93	20.38	4.81
% of cumulative	67.93	88.32	95.12
Oliwski Stream sediments with sweeping waste from gully tops			
Zn	0.610	−0.689	0.289
Cu	−0.633	0.348	0.692
Pb	0.494	−0.810	0.157
Cd	−0.925	−0.345	−0.152
Ni	−0.994	−0.111	−0.003
Cr	−0.954	−0.257	0.075
Fe	−0.880	−0.416	−0.126
Eigenvalue	4.55	1.62	0.63
% of variance	64.97	23.20	9.02
% of cumulative	64.97	88.18	97.20

Fig. 6. Cluster analysis based on Wards method (1r Pearson correlation) for HM in waste from the vehicle diagnostic station (V, TS, TB, WA).

Table 5
Rotated component matrix for principal component analysis loadings for HM in waste from the vehicle diagnostic station (V, TS, TB, WA).

Elements	Component		
	PC1	PC2	PC3
Zn	−0.647	−0.417	0.638
Cu	0.422	−0.845	−0.328
Pb	0.791	0.491	0.364
Cr	0.747	−0.654	−0.122
Cd	0.816	0.274	0.509
Ni	0.918	−0.378	0.121
Eigenvalue	3.44	2.42	1.13
% of variance	49.07	34.65	9.52
% of cumulative	49.07	83.73	93.25

suggest the tire wear source). Cu presented the quasi-independent behaviour with some correlation to PC1. Basing on the PC2 for MW loaded on Cu it could be stated that this element is supplemented into the RSW during vibration on uneven surfaces (or speed bumps) and extreme vehicle operation.

- In Grunwaldzka catchment the first group (PC1) was loaded on Cd, Ni, Cr, and Fe, which is in line with PC1 (Ni, Cd, Pb, Cr) for MW generated on all stages of vehicle diagnostic station. Therefore, the wearing out of car parts could be estimated as a source of these HMs on road surfaces and at the end in sediments of the stormwater receivers. For this catchment also separated Cu group was observed. Another possible source of this element was mentioned as leachates of Cu from roofs build of the copper plate (Nawrot and Wojciechowska, 2018). The PC3 for Grunwaldzka catchment was heavily loaded on Zn and in the same inversely correlated with PC1. The tire wear is the probable source of this element in RSW.

3.3.2. Pb isotope ratios

The ratios of stable isotopes ($^{206}Pb/^{207}Pb$, $^{208}Pb/^{206}Pb$, $^{208}Pb/^{207}Pb$) were measured to identify the sources of Pb in RSW and in MW. The minimum, maximum, and mean values of Pb isotopes are presented in Table S.4. The Pb isotopic ratios (Fig. 7a) for RSW ranged from 1.167 to 1.185 for $^{206}Pb/^{207}Pb$, from 2.046 to 2.070 for $^{208}Pb/^{206}Pb$, and from 2.401 to 2.450 for $^{208}Pb/^{207}Pb$, while in the case of MW the ratios were in the ranges of 1.152 to 1.165 for $^{206}Pb/^{207}Pb$, 2.050 to 2.085 for $^{208}Pb/^{206}Pb$, and 2.350 to 2.418 for $^{208}Pb/^{207}Pb$. The $^{206}Pb/^{207}Pb$ ratios for RSW and MW are significantly below the ratio characteristic for natural Pb, while the $^{208}Pb/^{206}Pb$ ratios for RSW and most MW were below 2.08. Only two samples of MW presented a higher $^{208}Pb/^{206}Pb = 2.08$ ratio which indicates that the Pb stemmed from gasoline (in places like the mechanical centre, this could be associated with servicing old vehicles). Nevertheless, except for the indicated case, the leaded and unleaded gasoline and diesel source of Pb could be excluded. Our observation indicate that the MW poses a separate source group of Pb (the points distribution for MW in Fig. 7a did not fall into any range). The Pb ratios of RSW depicted these waste as enriched with Pb from coal combustion sources. In Poland, heating systems are mainly coal-fired, which makes Poland the heaviest user of district heating systems and results in the highest air pollution in Europe (Wojdyga et al., 2014). The Pb isotopic ratios reported by Sutherland et al. (2003) for road deposited sediments in Palolo Valley, Oahu, Hawaii were in line with our results for RSW. They observed ratios in the ranges of 1.17–1.20 and 2.42–2.47 for $^{206}Pb/^{207}Pb$ and $^{208}Pb/^{207}Pb$, respectively. The MW ratios could bring information on the ranges of Pb sources from vehicle consumables (such as tyre wear, brake wear, etc.). Yu et al. (2016) reported ratios of $^{206}Pb/^{207}Pb$ from 1.14 to 1.16 and $^{208}Pb/^{206}Pb$ from 2.09 to 2.13 for vehicle exhaust, which is in line with the Pb isotopic ratios for MW. This confirms that car parts contribute to environmental contamination during exploitation. Fig. 7b presents the three isotopes ratios ($^{206}Pb/^{207}Pb$, $^{208}Pb/^{206}Pb$) for RSW and MW in relation to the Pb
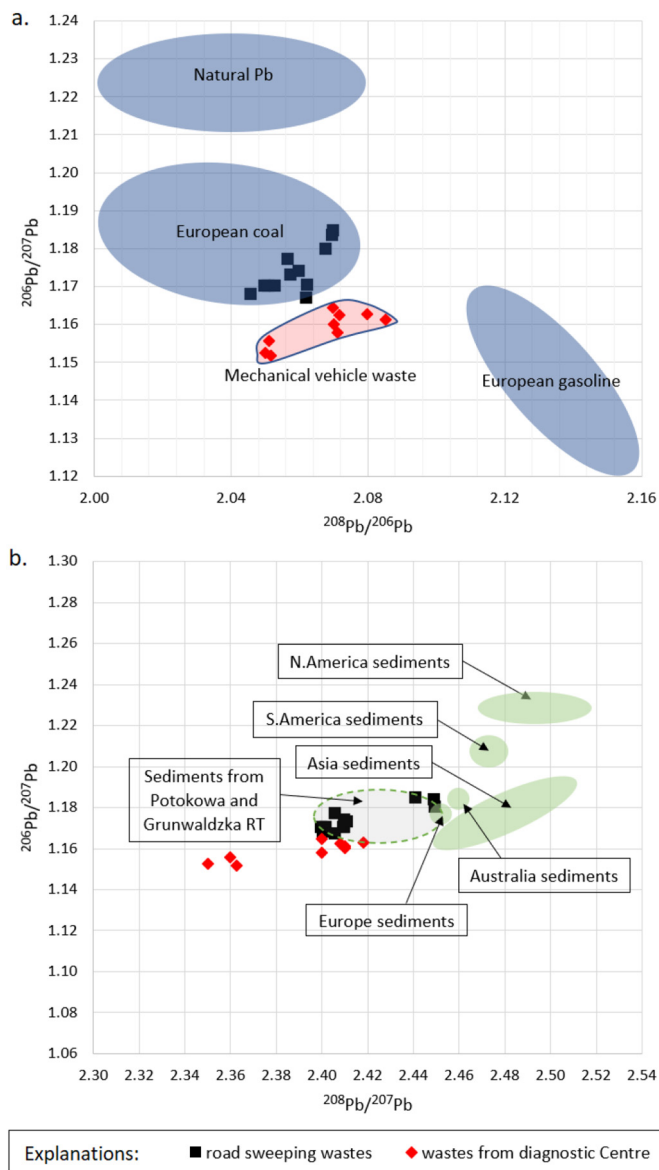

Fig. 7. a) A schematic three-isotope plot (Pb^{206}/Pb^{207} vs. Pb^{208}/Pb^{206}) showing the isotopic compositions of different Pb sources (Komárek et al., 2008; Zaborska, 2014) with the comparison of the results obtained for road sweeping waste (RSW) and mechanical waste (MW) from the diagnostic centre and b) a schematic three-isotope plot $^{206}Pb/^{207}Pb$ vs. $^{208}Pb/^{207}Pb$ diagram with isotopic ratios for sediments deposited in Potokowa and Grunwaldzka and major river sediments worldwide based on Millot and Alle (2004).

isotopic ratios for sediments deposited in Potokowa and Grunwaldzka as well as in relation to major river sediments worldwide (Millot and Alle, 2004). The results of Pb isotopes for RSW are in line with the results obtained for sediments from RTs and partly coincide with the river sediments in Europe described by Millot and Alle (2004). However, it is worth noting that sediments from Potokowa and Grunwaldzka RTs are at least partly composed of solids discharged from the stormwater drainage system therefore they present diverse Pb isotopic composition and ratios than river sediments.

3.3.3. Flag element ratio approach

The source tracking approach for Zn, Cu, Pb, Cd, Ni, and Cr in relation to reference Fe content is presented in Fig. 8. The red direction arrow is created by the results of metal concentrations for RSW collected from roads near the gully tops, which indicate the primary sources (the
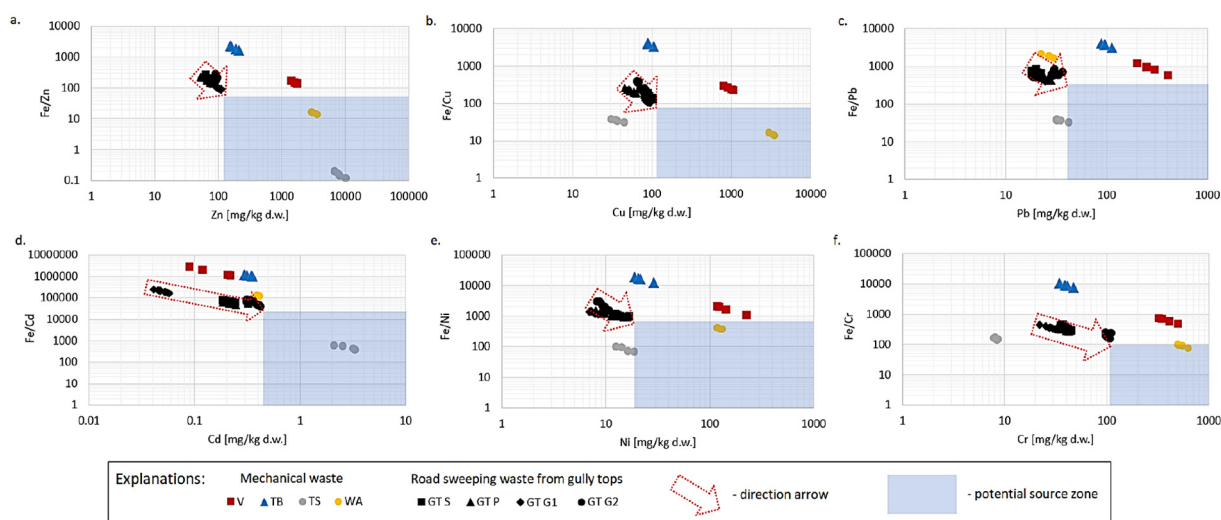
Fig. 8. Source tracking of a) Zn, b) Cu, c) Pb, d) Cd, e) Ni, f) Cr on road waste (waste from mechanical Centre: V – vulcanisation, TS – tyre scraps, TB – tyre balances, WA – wheeling alignment system for cars; road sweeping waste (RSW) collected from roads near the gully tops: GT S – Slowackiego gully top, Potokowa gully top, GT G1 – Grunwaldzka 1st gully top, GT G2 – Grunwaldzka 2nd gully top).

blue rectangle). It is worth noting that pollutant source particles generally described as primary sources are TS (Zn, Cd, and partly Ni and Pb) as well as WA (Zn, Cu, and partly Cr). These results confirm the important role of tyre wear and car usage in general for HMs supplementation (during brake wear, vehicle movement, shaking e.g. on rough roads or when not decelerating on speed bumps). The WA stage in vehicle centre simulate the real exploitation of vehicles on the roads. Moreover, the V and TB waste did not contribute HMs in urban roads, which means that HMs are retained in these stages at the mechanical centre. Besides, it is necessary to maintain proper waste management in such places. In research conducted by Hong et al. (2018), the authors indicated that Zn, Cu, Pb, Ni, and Cr are deposited on urban roads mainly by gasoline engine exhaust. For Cu release to the environment, brake lining dust was also indicated, while tyre wear was responsible for Zn release, which is in agreement with our results.

4. Conclusions

The contributions of road sweeping waste (RSW) and mechanical waste (MW) collected from the vehicle diagnostic centre to the contamination status of sediments deposited in urban retention tanks adjacent to heavy-traffic roads were assessed. We tested the connections and interactions between traffic-related wastes (RSW and MW) and bottom sediments of the urban retention tanks system.

The analyses of the seasonal distribution patterns of heavy metals (HM) in sediments indicated significant contamination in Potokowa and a moderate level in Grunwaldzka. Zn, Cu, Pb, Ni and Cr made the greatest contribution to sediment contamination. The HM concentrations observed in MW were significant (mean in mg/kg d.w.: 8444 for Zn in WA, 3308 for Cu in WA, 291 for Pb in V, 2.81 for Cd in TS, 154 for Ni in V, and 550 for Cr in WA). Zn, Cu, and Pb had a significant share in MW, while the HM content in RSW was at a similar level to the sediments. The total carcinogenic risk raises concerns due to the Cr content in MW and RWS. In general, the health risks evaluated in this study are within an acceptable range, although the risk caused by waste from vehicle diagnostic stations indicate a high risk of developing cancer for those in contact with this kind of waste. Special attention should be focused on Cr, Pb, and Ni.

A source tracking approach based on statistics (PCA) suggested that the HM in sediments could be divided into 3 groups of similar origin. For the Strzyza catchment they were: Zn-Pb-Ni-Cr-Fe as

mixed pathways of traffic and coal combustion, Cd with a concentration close to the geochemical background, and Cu which presented quasi-independent behaviour with some correlation to Zn-Pb-Ni-Cr-Fe. For the Grunwaldzka catchment, Cd-Ni-Cr were assessed as being emitted to the environment during the wearing of car parts; Cu presented unconventional behaviour and possibly originated from vehicle wear and tear or run-off from roofs covered with copper sheeting, while tyre wear was established as the probable source of the final Zn group. The Pb isotopic ratios of RSW established these waste as enriched with Pb from coal combustion sources, while the leaded and unleaded gasoline as well as diesel sources of Pb was excluded. This is in line with the significant air pollution in Poland; therefore, the metals correlated with Pb (Zn, Ni, Cr) in RSW and bottom sediments samples indicate the mixed pathways of their supplementation, including vehicle emission and coal combustion. The Pb isotopic ratios characteristic for MW are in the ranges of 1.152 to 1.165 for $^{206}Pb/^{207}Pb$, 2.050 to 2.085 for $^{208}Pb/^{206}Pb$, and 2.350 to 2.418 for $^{208}Pb/^{207}Pb$. These values indicate Pb sources from the wear of vehicle parts (such as tyre wear, brake wear, etc.). The source tracking results showed that waste associated with TS emit Zn, Cd and, to some extent, Ni and Pb onto road surfaces. The WA waste demonstrated the supplementation pathway for Zn, Cu, Ni, and partly Cr.

The complex analysis of HMs origin confirmed the motorization origin of analysed HMs. The results of various source tracking methods were coherent, but Pb isotope ratios alone brought important information allowing to link Pb in sediments to the atmospheric deposition of coal combustion products.

CRediT authorship contribution statement

N. Nawrot: Conceptualization, Methodology, Investigation, Visualization, Writing - original draft, Writing - review & editing. **E. Wojciechowska:** Supervision, Writing - review & editing. **S. Rezania:** Supervision. **J. Walkusz-Miotk:** Methodology, Validation. **K. Pazdro:** Supervision.

Declaration of competing interest

The authors declare that they have no known competing financial interests or personal relationships that could have appeared to influence the work reported in this paper.

Appendix A. Supplementary data

Supplementary data to this article can be found online at https://doi.org/10.1016/j.scitotenv.2020.141511.

References

Adamiec, E., Jarosz-Krzemińska, E., Wieszała, R., 2016. Heavy metals from non-exhaust vehicle emissions in urban and motorway road dusts. Environ. Monit. Assess. 188 (6). https://doi.org/10.1007/s10661-016-5377-1.

Agency for Toxic Substances and Disease Registry. Guidance for the preparation of a twenty first set toxicological profile. (2007). Available online: http://www.atsdr.cdc.gov/toxprofiles/guidance/set_21_ guidance.pdf (accessed on 21 April 2020).

Badach, J., Voordeckers, D., Nyka, L., Acker, M. Van, 2020. A framework for air quality management zones – useful GIS-based tool for urban planning: case studies in Antwerp and Gdańsk. Build. Environ. 174 (December 2019), 106743. https://doi.org/10.1016/j.buildenv.2020.106743.

Cai, L., Xu, Z., Ren, M., Guo, Q., Hu, X., Hu, G., 2012. Source identification of eight hazardous heavy metals in agricultural soils of. Ecotoxicol. Environ. Saf. 78, 2–8. https://doi.org/10.1016/j.ecoenv.2011.07.004.

Chabukdhara, M., Nema, A.K., 2013. Heavy metals assessment in urban soil around industrial clusters in Ghaziabad, India: probabilistic health risk approach. Ecotoxicol. Environ. Saf. 87, 57–64. https://doi.org/10.1016/j.ecoenv.2012.08.032.

Chrastný, V., Šillerová, H., Vítková, M., Francová, A., Jehlička, J., Kocourková, J., Aspholm, P.E., Nilsson, L.O., Berglen, T.F., Jensen, H.K.B., Komárek, M., 2018. Unleaded gasoline as a significant source of Pb emissions in the Subarctic. Chemosphere 193, 230–236. https://doi.org/10.1016/j.chemosphere.2017.11.031.

Crosby, C.J., Fullen, M.A., Booth, C.A., Searle, D.E., 2014. A dynamic approach to urban road deposited sediment pollution monitoring (Marylebone Road, London, UK). J. Appl. Geophys. 105, 10–20. https://doi.org/10.1016/j.jappgeo.2014.03.006.

Ferreira, A.J.D., Soares, D., Serrano, L.M.V., Walsh, R.P.D., Dias-Ferreira, C., Ferreira, C.S.S., 2016. Roads as sources of heavy metals in urban areas. The Covões catchment experiment, Coimbra, Portugal. J. Soils Sediments 16 (11), 2622–2639. https://doi.org/10.1007/s11368-016-1492-4.

González-Macías, C., Sánchez-Reyna, G., Salazar-Coria, L., Schifter, I., 2014. Application of the positive matrix factorization approach to identify heavy metal sources in sediments. A case study on the Mexican Pacific Coast. Environ. Monit. Assess. 186, 307–324. https://doi.org/10.1007/s10661-013-3375-0.

Hakanson, L., 1980. An ecological risk index for aquatic pollution control. A sedimentological approach. Water Res. 14, 975–1001. https://doi.org/10.1016/0043-1354(80)90143-8.

Hanif, N., Eqani, S.A.M.A.S., Ali, S.M., Cincinelli, A., Ali, N., Katsoyiannis, I.A., ... Bokhari, H., 2016. Geo-accumulation and enrichment of trace metals in sediments and their associated risks in the Chenab River, Pakistan. Journal of Geochemical Exploration 165, 62–70. https://doi.org/10.1016/j.gexplo.2016.02.006.

Hong, N., Zhu, P., Liu, A., Zhao, X., Guan, Y., 2018. Using an innovative flag element ratio approach to tracking potential sources of heavy metals on urban road surfaces*. Environ. Pollut. 243, 410–417. https://doi.org/10.1016/j.envpol.2018.08.098.

https://pl.climate-data.org/ - data for Gdansk, Pomeranian Voivodeship, accessed on 1st July 2020.

Hu, X., Zhang, Y., Ding, Z., Wang, T., Lian, H., Sun, Y., Wu, J., 2012. Bioaccessibility and health risk of arsenic and heavy metals (Cd, Co, Cr, Cu, Ni, Pb, Zn and Mn) in TSP and PM2.5 in Nanjing, China. Atmos. Environ. 57, 146–152. https://doi.org/10.1016/j.atmosenv.2012.04.056.

IRIS (Integrated Risk Information System) Assessment by US EPA. https://cfpub.epa.gov/ncea/iris_drafts/AtoZ.cfm. (Accessed 1 May 2020).

Islam, S., Ahmed, K., Habibullah-Al-Mamun, M., Masunaga, S., 2015a. Potential ecological risk of hazardous elements in different land-use urban soils of Bangladesh. Sci. Total Environ. 512–513, 94–102. https://doi.org/10.1016/j.scitotenv.2014.12.100.

Islam, M.S., Ahmed, M.K., Raknuzzaman, M., Habibullah -Al- Mamun, M., Islam, M.K., 2015b. Heavy metal pollution in surface water and sediment: a preliminary assessment of an urban river in a developing country. Ecol. Indic. 48, 282–291. https://doi.org/10.1016/j.ecolind.2014.08.016.

Kamunda, C., Mathuthu, M., Madhuku, M., 2016. Health risk assessment of heavy metals in soils from Witwatersrand Gold Mining Basin, South Africa. Int. J. Environ. Res. Public Health 13 (7), 663. https://doi.org/10.3390/ijerph13070663.

Komárek, M., Chrastný, V., Mihaljevi, M., 2008. Lead isotopes in environmental sciences: a review. Environ. Int. 34, 562–577. https://doi.org/10.1016/j.envint.2007.10.005.

Kowalska, J.B., Mazurek, R., Gąsiorek, M., Zaleski, T., 2018. Pollution indices as useful tools for the comprehensive evaluation of the degree of soil contamination–a review. Environ. Geochem. Health, 1–26 https://doi.org/10.1007/s10653-018-0106-z.

Kundzewicz, Z.W., Piniewski, M., Mezghani, A., Okruszko, T., Pińskwar, I., Kardel, I., Hov, Ø., Szczęśniak, M., Szwed, M., Benestad, R.E., Marcinkowski, P., Graczyk, D., Dobler, A., Førland, E.J., O'Keefe, J., Choryński, A., Parding, K.M., Haugen, J.E., 2018. Assessment of climate change and associated impact on selected sectors in Poland. Acta Geophysics 66, 1509–1523. https://doi.org/10.1007/s11600-018-0220-4.

Luo, X., Ding, J., Xu, B., Wang, Y., Li, H., Yu, S., 2012. Incorporating bioaccessibility into human health risk assessments of heavy metals in urban park soils. Sci. Total Environ. 424, 88–96. https://doi.org/10.1016/j.scitotenv.2012.02.053.

Mandeng, B., Bondj, L.M., Zacharie, A., Bessa, E., Ntomb, Y.D., Wadjou, J.W., ... Dieudonn, L.B., 2019. Contamination and risk assessment of heavy metals, and uranium of sediments in two watersheds in Abiete-Toko gold district, Southern Cameroon. Heliyon 5 (10), e02591. https://doi.org/10.1016/j.heliyon.2019.e02591 Oct.

Men, C., Liu, R., Wang, Q., Guo, L., Shen, Z., 2018. The impact of seasonal varied human activity on characteristics and sources of heavy metals in metropolitan road dusts. Sci. Total Environ. 637–638, 844–854. https://doi.org/10.1016/j.scitotenv.2018.05.059.

Millot, R., Alle, C., 2004. Lead isotopic systematics of major river sediments: a new estimate of the Pb isotopic composition of the Upper Continental Crust. Chem. Geol. 203, 75–90. https://doi.org/10.1016/j.chemgeo.2003.09.002.

Nawrot, N., Wojciechowska, E., 2018. Assessment of trace metals leaching during rainfall events from building rooftops with different types of coverage – case study. Journal of Ecological Engineering 19 (3). https://doi.org/10.12911/22998993/85410.

Nawrot, N., Wojciechowska, E., Matej-Łukowicz, K., Walkusz-Miotk, J., Pazdro, K., 2019. Spatial and vertical distribution analysis of heavy metals in urban retention tanks sediments: a case study of Strzyza stream. Environ. Geochem. Health 8. https://doi.org/10.1007/s10653-019-00439-8.

Pant, P., Harrison, R.M., 2013. Estimation of the contribution of road traffic emissions to particulate matter concentrations from field measurements: a review. Atmos. Environ. 77, 78–97. https://doi.org/10.1016/j.atmosenv.2013.04.028.

Qing, X., Yutong, Z., Shenggao, L., 2015. Assessment of heavy metal pollution and human health risk in urban soils of steel industrial city (Anshan), Liaoning, Northeast China. Ecotoxicol. Environ. Saf. 120, 377–385. https://doi.org/10.1016/j.ecoenv.2015.06.019.

Sakson, G., Brzezinska, A., Zawilski, M., 2018. Emission of heavy metals from an urban catchment into receiving water and possibility of its limitation on the example of Lodz city. Environ. Monit. Assess. 190. https://doi.org/10.1007/s10661-018-6648-9.

Shi, G., Chen, Z., Bi, C., Wang, L., Teng, J., Li, Y., Xu, S., 2011. A comparative study of health risk of potentially toxic metals in urban and suburban road dust in the most populated city of China. Atmos. Environ. 45 (3), 764–771. https://doi.org/10.1016/j.atmosenv.2010.08.039.

Sojka, M., Jaskula, J., Siepak, M., 2018. Heavy metals in bottom sediments of reservoirs in the lowland area of western Poland: concentrations, distribution, sources and ecological risk. Water (Switzerland) 11, 1–20. https://doi.org/10.3390/w11010056.

Sun, J., Yu, R., Hu, G., Su, G., Zhang, Y., 2018. Catena tracing of heavy metal sources and mobility in a soil depth profile via isotopic variation of Pb and Sr. Catena 171 (February), 440–449. https://doi.org/10.1016/j.catena.2018.07.040.

Sun, L., Guo, D., Liu, K., Meng, H., Zheng, Y., Yuan, F., Zhu, G., 2019. Catena levels, sources, and spatial distribution of heavy metals in soils from a typical coal industrial city of Tangshan, China. Catena 175 (July 2018), 101–109. https://doi.org/10.1016/j.catena.2018.12.014.

Sutherland, R.A., Day, J.P., Bussen, J.O., 2003. Lead concentrations, isotope ratios, and source apportionment in road deposited sediments, Honolulu, Oahu, Hawaii. Water Air Soil Pollut. 142 (1–4), 165–186. https://doi.org/10.1023/A:1022026612922.

Sýkorová, I., Havelcová, M., Trejtnarová, H., Kotlík, B., 2012. Toxicologically important trace elements and organic compounds investigated in size-fractionated urban particulate matter collected near the Prague highway. Sci. Total Environ. 437, 127–136. https://doi.org/10.1016/j.scitotenv.2012.07.030.

Tomlinson, D.L., Wilson, J.G., Harris, C.R., Jeffrey, D.W., 2013. Assessment of heavy metal enrichment and degree of contamination around the copper-nickel mine in the Selebi Phikwe Region, Eastern Botswana. Environ. Ecol. Res. 1 (2), 32–40. https://doi.org/10.13189/eer.2013.010202.

Unda-Calvo, J., Ruiz-Romera, E., Vallejuelo, S.F. De, Martínez-santos, M., Gredilla, A., 2019. Evaluating the role of particle size on urban environmental geochemistry of metals in surface sediments. Sci. Total Environ. 646, 121–133. https://doi.org/10.1016/j.scitotenv.2018.07.172.

US EPA, 1989. Risk assessment guidance for superfund (RAGS). Human Health Evaluation Manual (HHEM) — Part A, Baseline Risk Assessment. vol. I. Office of Emergency and Remedial Response, Washington DC (EPA/540/1-89/002).

US EPA, 2001. Risk Assessment Guidance for Superfund: Volume III — Part A, Process for Conducting Probabilistic Risk Assessment. US Environmental Protection Agency, Washington, DC (EPA 540-R-02-002).

Wang, Y., Yang, L., Kong, L., Liu, E., Wang, L., Zhu, J., 2015. Spatial distribution, ecological risk assessment and source identification for heavy metals in surface sediments from Dongping Lake, Shandong. East China. Catena 125, 200–205. https://doi.org/10.1016/j.catena.2014.10.023.

Wang, S., Cai, L., Wen, H., Luo, J., Wang, Q., Liu, X., 2019. Spatial distribution and source apportionment of heavy metals in soil from a typical county-level city of Guangdong Province, China. Sci. Total Environ. 655, 92–101. https://doi.org/10.1016/j.scitotenv.2018.11.244.

Wei, X., Gao, B., Wang, P., Zhou, H., Lu, J., 2015. Pollution characteristics and health risk assessment of heavy metals in street dusts from different functional areas in Beijing, China. Ecotoxicol. Environ. Saf. 112, 186–192. https://doi.org/10.1016/j.ecoenv.2014.11.005.

Wojciechowska, E., Nawrot, N., Walkusz-Miotk, J., Matej-Łukowicz, K., Pazdro, K., 2019. Heavy metals in sediments of urban streams: contamination and health risk assessment of influencing factors. Sustainability 11, 563. https://doi.org/10.3390/su11030563.

Wojdyga, K., Chorzelski, M., Rozycka-Wronska, E., 2014. Emission of pollutants in flue gases from polish district heating sources. J. Clean. Prod. 75, 157–165. https://doi.org/10.1016/j.jclepro.2014.03.069.

Wu, P., Yin, A., Yang, X., Zhang, H., Fan, M., Gao, C., 2017. Distribution and source identification of heavy metals in the sediments of a river flowing an urbanization gradient, eastern China. Environ. Earth Sci. 76 (21), 1–11. https://doi.org/10.1007/s12665-017-7068-9.

Yang, Z., Lu, W., Long, Y., Bao, X., Yang, Q., 2011. Assessment of heavy metals contamination in urban topsoil from Changchun City, China. J. Geochem. Explor. 108 (1), 27–38. https://doi.org/10.1016/j.gexplo.2010.09.006.

Yao, P.H., Shyu, G.S., Chang, Y.F., Chou, Y.C., Shen, C.C., Chou, C.S., Chang, T.K., 2015. Lead isotope characterization of petroleum fuels in Taipei, Taiwan. Int. J. Environ. Res. Public Health 12, 4602–4616. https://doi.org/10.3390/ijerph120504602.

Yu, Y., Li, Y., Li, B., Shen, Z., Stenstrom, M.K., 2016. Metal enrichment and lead isotope analysis for source apportionment in the urban dust and rural surface soil. Environ. Pollut. 216, 764–772. https://doi.org/10.1016/j.envpol.2016.06.046.

Yuen, J.Q., Olin, P.H., Lim, H.S., Benner, S.G., Sutherland, R.A., Ziegler, A.D., 2012. Accumulation of potentially toxic elements in road deposited sediments in residential and light industrial neighborhoods of Singapore. J. Environ. Manag. 101, 151–163. https://doi.org/10.1016/j.jenvman.2011.11.017.

Zaborska, A., 2014. Anthropogenic lead concentrations and sources in Baltic Sea sediments based on lead isotopic composition. Mar. Pollut. Bull. 85 (1), 99–113. https://doi.org/10.1016/j.marpolbul.2014.06.013.

Zaborska, A., Zawierucha, K., 2016. Chemosphere accumulation of atmospheric radionuclides and heavy metals in cryoconite holes on an Arctic glacier. Chemosphere 160, 162–172. https://doi.org/10.1016/j.chemosphere.2016.06.051.

Zafra, C., Temprano, J., Tejero, I., 2017. The physical factors affecting heavy metals accumulated in the sediment deposited on road surfaces in dry weather: a review. Urban Water J. 9006, 1–11. https://doi.org/10.1080/1573062X.2016.1223320.

Zemełka, G., Kryłów, M., Szalińska van Overdijk, E., 2019. The potential impact of land use changes on heavy metal contamination in the drinking water reservoir catchment (Dobczyce Reservoir, south Poland). Archives of Environmental Protection 45 (2), 3–11. https://doi.org/10.24425/aep.2019.127975.

Zgłobicki, W., Telecka, M., Skupiński, S., 2019. Assessment of short-term changes in street dust pollution with heavy metals in Lublin (E Poland) — levels, sources and risks. Environ. Sci. Pollut. Res. 26 (2019), 35049–35060. https://doi.org/10.1007/s11356-019-06496-x.

Zhang, J., Hua, P., Krebs, P., 2017. Influences of land use and antecedent dry-weather period on pollution level and ecological risk of heavy metals in road-deposited sediment. Environ. Pollut. 228, 158–168. https://doi.org/10.1016/j.envpol.2017.05.029.

Zhao, L., Xu, Y., Hou, H., Shangguan, Y., Li, F., 2014. Source identification and health risk assessment of metals in urban soils around the Tanggu chemical industrial district, Tianjin, China. Sci. Total Environ. 468–469, 654–662. https://doi.org/10.1016/j.scitotenv.2013.08.094.